9 March 2001

ELSEVIER

Chemical Physics Letters 336 (2001) 109–117

CHEMICAL PHYSICS LETTERS

www.elsevier.nl/locate/cplett

An investigation of N_2O production from quenching of $OH(A\,^2\Sigma^+)$ by N_2

E.G. Estupiñán [a], R.E. Stickel [a], P.H. Wine [a,b,*]

[a] *School of Earth and Atmospheric Sciences, Georgia Institute of Technology, Atlanta, GA 30332-0340, USA*
[b] *School of Chemistry and Biochemistry, Georgia Institute of Technology, Atlanta, GA 30332-0400, USA*

Received 5 October 2000; in final form 21 December 2000

Abstract

Production of N_2O from collisional quenching of electronically excited $OH(A\,^2\Sigma^+)$ by N_2 was investigated in order to establish the importance of this process in the atmospheric budget of N_2O. The experimental approach, sequential pulsed laser production and excitation of OH combined with N_2O detection by tunable diode laser absorption spectroscopy, minimizes interferences from potential artifact sources of N_2O. The quantum yield for production of N_2O is found to be less than 1×10^{-4}, i.e., more than 100 times lower than the threshold for atmospheric importance. © 2001 Published by Elsevier Science B.V.

1. Introduction

Nitrous oxide (N_2O) is an important trace gas in the Earth's atmosphere. Its contribution to the greenhouse effect is considerable due to its long residence time of about 150 years and the relatively large energy absorption capacity per molecule [1]. Nitrous oxide is inert in the troposphere. However, in the stratosphere, especially in the middle and upper stratosphere, N_2O is destroyed by photolysis (~90%) and by reaction with electronically excited $O(^1D_2)$ atoms (~10%) [2]. The oxidation of N_2O by $O(^1D_2)$ forms NO, and represents the dominant source of total reactive nitrogen (NO_y) in the stratosphere [3].

Even though uncertainties in the source and sink budget of atmospheric N_2O remain large [3–6], it is widely accepted that major sources all introduce N_2O into the atmosphere near the earth's surface [7]. The possible existence of in situ atmospheric sources of N_2O is still a controversial subject, although laboratory studies are reported in the literature that provide evidence for the existence of such sources [8–10].

Isotopic composition studies provide useful constraints on the global sources and sinks of atmospheric nitrous oxide [11–16]. One important aspect that these studies have revealed is that atmospheric N_2O samples show a mass-independent heavy oxygen isotope effect, i.e., an anomalous ratio of $N_2{}^{17}O$-to-$N_2{}^{18}O$ concentration ratio, which increases with altitude (or distance from known sources) [12,15]. Calculations by Miller and Yung [17,18] predict that N_2O UV photolysis in the stratosphere selectively destroys 'light N_2O', thus leaving behind N_2O that is enriched in the

* Corresponding author. Fax: +1-404-894-6285.
E-mail address: paul.wine@chemistry.gatech.edu (P.H. Wine).

0009-2614/01/$ - see front matter © 2001 Published by Elsevier Science B.V.
PII: S0009-2614(01)00082-3

heavier isotopes of both N and O. Recent laboratory experiments [19–21] support the predictions of Miller and Yung, and recent field observations [14,16] are also consistent with the magnitude of the enrichments in $^{14}N^{14}N^{18}O$, $^{14}N^{15}N^{16}O$, and $^{15}N^{14}N^{16}O$ predicted by the Miller and Yung theory. However, N_2O photolysis is a mass-dependent process [15,18] and, therefore, does not account for the mass-independent fractionation in N_2O.

This work evaluates the possible formation of N_2O from electronically excited OH:

$$OH(X^2\Pi) + h\nu(\lambda \sim 308\ \text{nm}) \rightarrow OH(A^2\Sigma^+). \quad (1)$$

$$OH(A^2\Sigma^+) + N_2 \rightarrow OH(X^2\Pi) + N_2 \quad (2a)$$

$$\rightarrow N_2O + H. \quad (2b)$$

If k_{2b}/k_2 is relatively large, i.e., greater than 0.01, then the rate of solar excitation of the 0–0 band of the $A^2\Sigma^+ \leftarrow X^2\Pi$ transition of OH at $\lambda \sim 308$ nm is sufficiently large that reaction (2b) could be a significant source of atmospheric N_2O. In addition, atmospheric OH is generated from O_3:

$$O_3 + h\nu \rightarrow O(^1D_2) + O_2(a^1\Delta_g) \quad (3a)$$

$$\rightarrow O(^3P_J) + O_2(X^3\Sigma_g^-) \quad (3b)$$

$$\rightarrow \text{spin-forbidden products.} \quad (3c)$$

$$O(^1D_2) + H_2O \rightarrow 2OH. \quad (4)$$

Since stratospheric O_3 is characterized by a mass-independent enrichment of the heavy oxygen isotopes [22], the possibility that the mass-independent N_2O enrichment comes from O_3 via reactions (1)–(4) warrants investigation. Further support for the potential importance of reaction (2b) in atmospheric chemistry comes from studies of the (reverse) reaction of translationally hot H atoms with N_2O, where chemiluminescence from $OH(A^2\Sigma^+)$ is observed [23–25] although, unfortunately, the yield of $OH(A^2\Sigma^+)$ is not reported. When H atoms are produced from 193 nm photolysis of HBr under bulk conditions, where all collision geometries occur, nearly half of the observed $OH(A^2\Sigma^+)$ is vibrationally excited [23]. When H atoms are produced by photodissociation of HBr–N_2O complexes in molecular beams, thus restricting the angle of attack of H on N_2O, the $OH(A^2\Sigma^+)$ product is observed to have less vibrational excitation but more rotational excitation than under bulk conditions [25].

Although no experimental studies of reaction (2b) are reported in the peer-reviewed literature, evidence for its occurrence was reported informally during the early 1980s [26]. This stimulated a study where an attempt was made to observe N_2O production in an experiment where OH was produced in the presence of N_2 in a low-pressure discharge flow apparatus and excited to the $A^2\Sigma^+$ state using an arc lamp [27]. Unfortunately, production of N_2O from poorly controlled background sources swamped any N_2O that may have been generated via reaction (2b), so the occurrence of this reaction with an atmospherically relevant yield could be neither demonstrated nor ruled out. The approach employed in this study minimizes artifact sources of N_2O, thus allowing the potential atmospheric importance of reaction (2b) to be assessed.

2. Experimental technique

A schematic diagram of the experimental apparatus is shown in Fig. 1. Electronically excited OH was produced by optical excitation of ground state OH radicals that were generated by laser flash photolysis of H_2O_2/N_2 mixtures in a static cell equipped with anti-reflection (AR) coated windows (248–355 nm). Tunable diode laser absorption spectroscopy (TDLAS) in a connected multipass cell with internal mirrors was used for N_2O detection.

The reaction cell was a Pyrex cylinder 25 mm in diameter and 68 cm in length with o-ring joints for attaching the windows. Hydroxyl radicals were produced by 248 nm laser flash photolysis of H_2O_2. A Lambda Physik Compex 102 KrF excimer laser operating at a repetition rate of 5 Hz served as the photolytic source; the laser pulse width was approximately 30 ns (FWHM). A 5 mm diameter aperture selected the central, most intense, and most spatially uniform portion of the photolysis beam, and also restricted the volume photolyzed by the laser (which minimized the destruction rate of H_2O_2). The laser power exiting

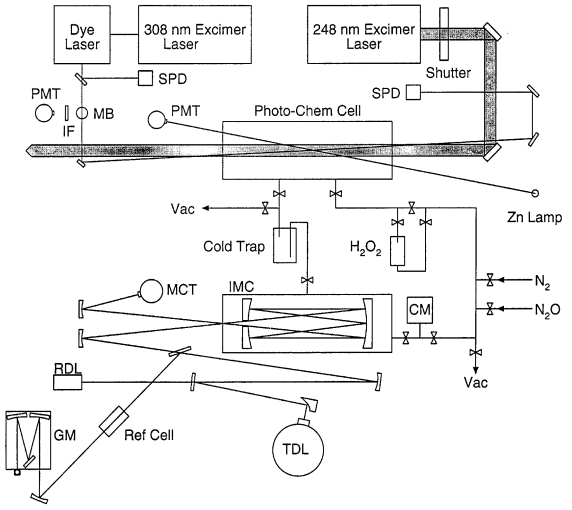

Fig. 1. Apparatus for studying the $OH(A^2\Sigma^+) + N_2$ reaction: TDL = tunable diode laser; IMC = infrared multipass cell; MCT = HgCdTe detector; RDL = red diode laser; Photo-Chem Cell = photochemistry cell; SPD = Si photodiode, PMT = photomultiplier tube; CM = capacitance manometer; GM = grating monochromator with MCT; IF = interference filter; MB = Meeker burner.

the photolysis cell was typically 18 mJ/pulse. H_2O_2 was introduced into the photolysis cell by slowly flowing gaseous N_2 through liquid H_2O_2 in a Pyrex bubbler held at 265 K to minimize the amount of H_2O admitted to the cell.

A pulsed, frequency-doubled tunable dye laser (Lambda Physik model LPD 3000) was employed to excite OH to the $A^2\Sigma^+$ state. The dye laser was pumped with 308 nm radiation from a Lambda Physik model Lextra-MC excimer laser. The pulse width of the frequency-doubled dye laser was approximately 20 ns (FWHM), the beam diameter was approximately 3 mm, and the pulse energy ranged from 10 to 150 μJ. The dye laser beam passed through the photolysis cell in the opposite direction to the 248 nm beam, and traversed the volume photolyzed by the 248 nm beam down the entire length of the cell. The two pulsed laser beams were synchronized in time such that the dye laser beam traversed the cell 1.5 μs after the 248 nm beam; loss of ground state OH by reaction with H_2O_2 was unimportant on this time scale. Observation of laser-induced fluorescence from OH radicals in a burner flame was employed to locate and assign OH absorption features in the 0–0 band of the $A^2\Sigma^+ \leftarrow X^2\Pi$ system at $\lambda \sim 308$ nm. The OH spectrum reported by Diecke and Crosswhite [28] was used as a basis for the assignments.

The dye laser power of each laser shot was monitored by two silicon photodiodes, positioned near the two ends of the reaction cell, which sampled a small fraction of the beam reflected off uncoated quartz plates. The first photodiode, which was positioned between the reaction cell and the dye laser, was absolutely calibrated by comparing the photodiode readings with those measured by a Scientech model 214 disk calorimeter. This calibration was corrected for window losses and reflections. The second photodiode, positioned at the dye laser exit from the photolysis cell, permitted the evaluation of the number of $OH(A^2\Sigma^+)$ molecules generated by each laser shot through direct measurement of the absorption of dye laser radiation by $OH(X^2\Pi)$ molecules. A shutter placed between the excimer laser and the photolysis cell allowed the second photodiode to monitor the dye laser power exiting the reaction cell under conditions where no OH molecules were present in the reaction cell (I_0). The shutter was programmed to stay closed 10% of the time of irradiation (for measurement of I_0) and to stay open 90% of the time of irradiation (for measurement of I, the transmitted dye laser intensity with OH radicals present in the beam path). The difference $I_0 - I$ directly gives the number of $OH(A^2\Sigma^+)$ produced (if I_0 and I are expressed in units of photons).

The concentration of H_2O_2 in the reaction cell was monitored by UV photometry at 213.9 nm (Zn penray lamp light source). The lamp radiation crossed the reaction cell diagonally. A band-pass filter at 213.9 nm isolated a region of strong H_2O_2 absorption and a UV-sensitive photomultiplier tube monitored the light level.

To prevent damage of the mirrors in the infrared multipass cell by H_2O_2, a Pyrex trap cooled to dry ice temperature (195 K) was placed between the photolysis cell and the infrared multipass cell. It was demonstrated experimentally that N_2O at the concentrations of interest could be quantitatively transferred through the trap from one cell to the other.

Nitrous oxide was monitored at 2207 cm^{-1} using highly monochromatic infrared radiation from a lead salt tunable diode laser housed in a liquid nitrogen cooled Dewar. Details of the infrared N_2O detection system can be found elsewhere [29].

The pressure in the photolysis cell, the light level reaching the photomultiplier tube monitoring H_2O_2 concentrations, the signal from both photodiodes, and the ratio of the two digitized first harmonic signals from the IR detection system were all digitized and fed into an MS-DOS compatible microcomputer, where the information was stored for later analysis.

The N_2 used in this study was UHP grade with a stated minimum purity of 99.999%; it was used as supplied. The N_2O calibration gas was a certified standard containing 0.969 ppmv N_2O in UHP N_2. The liquid H_2O_2 sample was 50 wt% in H_2O, but it was concentrated by bubbling N_2 through it for several days before experiments were undertaken. The H_2O_2 bubbler was cooled to $-8°C$ to minimize the amount of water vapor introduced into the photolysis cell.

3. Results and discussion

All experiments were carried out under static-fill conditions. Figs. 2 and 3 show typical experimental results (experiment 9 in Table 1). Fig. 2 shows how the concentration of N_2O, as measured in the multipass infrared absorption cell, varied over the course of an experiment. Fig. 3 shows how the concentration of H_2O_2 and the number of $OH(A^2\Sigma^+)$ molecules generated per dye laser shot varied as a function of the total (integrated) number of 248 nm photons absorbed by H_2O_2 over the course of the experiment. The experimental procedure employed to obtain the data shown in Figs. 2 and 3 is discussed below.

Before the experiment was started, both cells were pumped out, and the transmitted light intensity (I_0) at 213.9 nm was measured. At $t = 0$, the multipass cell was filled to 42 Torr with 0.969 ppmv N_2O standard mixture and its absorption was measured. About 2 min later, the multipass cell was pumped out and the background absorption was obtained for the next 7 min by pumping on the cell. At the same time, N_2 was slowly flowed through the H_2O_2 bubbler until the pressure in the photolysis cell reached 108 Torr. While the cell was being filled to this final pressure, the valve between the reaction cell and the trap was kept closed to prevent H_2O_2 from passing into the multipass cell. The irradiation was then started in the reaction cell and stopped 30 min later when the H_2O_2 concentration had dropped by about a

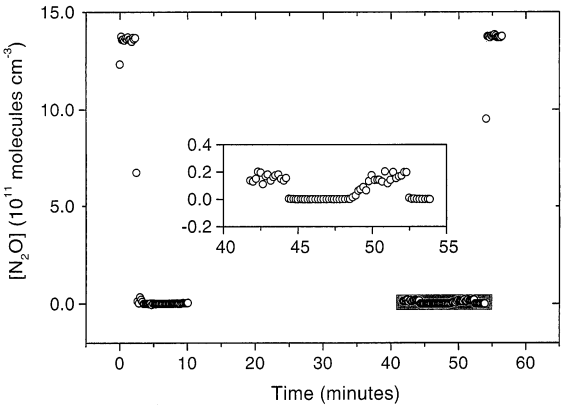

Fig. 2. Plot showing the time history of N_2O concentration measurements made over the course of experiment no. 9 (Table 1). Details of the experimental procedure and data interpretation are given in the text.

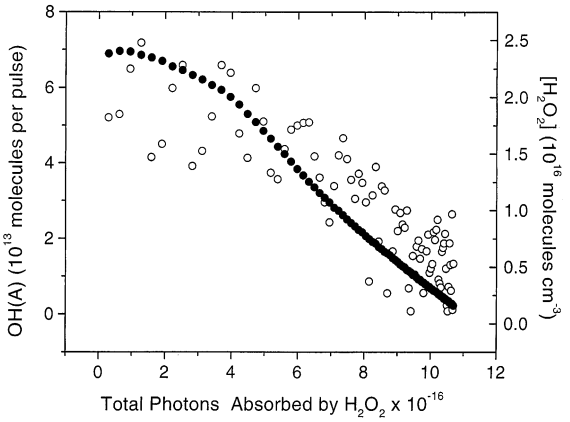

Fig. 3. Plot of the number of $OH(A^2\Sigma^+)$ molecules generated per dye laser shot (empty circles) and $[H_2O_2]$ (filled circles) versus the cumulative number of photons absorbed by H_2O_2 in the same experiment shown in Fig. 2. Each data point represents a 20 second average.

Table 1
Summary of experimental results[a]

Experiment no.	Average excimer laser power (mJ/pulse)	Average dye laser power (mJ/pulse)	Irradiation time (min)	Total N_2O detected (10^{12} molecules)	Photolytic N_2O detected (10^{12} molecules)	$OH(A^2\Sigma^+)$ generated (10^{17} molecules)	Raw N_2O yield (10^{-5})	Net N_2O yield (10^{-5})
1	20	0.12	25	5.5	2.8	2.8	3.0	1.5
2	20	0.10	18	0.0	−2.7	1.9	0.0	0.0
3[b]	20	0.10	22	2.7				
4	18	0.10	27	4.3	5.7	3.0	2.1	2.9
5[b]	18	0.08	28	−1.4				
6	18	0.07	23	−1.4	−1.4	2.0	−1.1	−1.1
7	18	0.05	20	0.0	0.0	1.5	0.0	0.0
8	18	0.05	23	0.0	0.0	1.9	0.0	0.0
9	18	0.04	30	1.5	1.5	2.2	1.0	1.0
10[b]	18	0.01	25	0.0				
11	9	0.04	29	0.0	0.0	0.7	0.0	0.0
12	5	0.03	29	−4.6	−4.6	0.5	−13.2	−13.2
13[b]	18	0.02	30	0.0				
14[c]	18	0.02	18	233		0.4		
15[d]	18	0.02	20	121		0.6		
16[e]	17	0.15	22	8.1	4.1	0.4	27.8	13.8
17[f]	17	0.13	17	−1.3	−5.4	0.1	−15.5	−62.6
18[b]	17	0.08	18	4.1				
19	0	0	30	9.9				
20	0	0	30	6.9				
21[g]	16	0.11	27	6.9	5.4	3.8	2.1	2.1
22[b,g]	16	0.12	26	1.5				

[a] Unless otherwise noted, experiments were performed at a total pressure of about 105 Torr, the buffer gas was N_2, and ground state OH was excited via the $Q_1(2)$ line.
[b] Ground state OH not excited, i.e., dye laser tuned off an OH line.
[c] 215 ppb of N_2O were added to the initial mixture and 233 ± 18 ppb were detected. Error is at the 2σ level and represents precision only.
[d] 121 ppb of N_2O were added to the initial mixture and 121 ± 16 ppb were detected. Error is at the 2σ level and represents precision only.
[e] OH was excited via the $Q_1(6)$ line.
[f] OH was excited via the $Q_1(7)$ line.
[g] Ar buffer gas.

factor of 15. For this particular experiment, the dye laser was tuned to the strong $Q_1(2)$ OH absorption line. As depicted in Fig. 3, the concentration of H_2O_2 decreased over the irradiation period as the laser photolyzed H_2O_2; losses to the walls of the reaction cell also contributed to the drop in H_2O_2 concentration. At $t = 42$ min, the laser irradiations were stopped and the valve between the two cells was opened so the reaction products could expand into the infrared multipass cell (reducing the total pressure to 45 Torr). About 2.5 min later, i.e., after a measurement of N_2O was completed, the multipass cell was pumped out and a background absorption measurement (pumping on the cell) was obtained for the next 3 min. A second background measurement was taken for about 2 minutes by adding N_2 to the multipass cell (at approximately the same rate that N_2/H_2O_2 was added to the reaction cell) and measuring the N_2O content. This second background reading was taken because it was observed that a small N_2O signal was detected even when only N_2 was introduced into the multipass cell. As shown in the expanded scale inset in Fig. 2, the N_2O signal observed with only N_2 added is similar in magnitude to the signal observed after the reaction

products were expanded into the detection cell. On average, this was the case for all experiments. Possible sources of background N_2O include the N_2 gas cylinder, heterogeneous chemistry in the regulator on the N_2 cylinder, and/or small leaks of atmospheric N_2O into the cell. At the end of the experiment, the absorption from the N_2O standard mixture was again measured. Only a trace of N_2O, if any, was found to be produced photochemically from this experiment (Fig. 2).

Table 1 summarizes the conditions and results from the 22 experiments that were performed to study the N_2O yield from the reactive quenching of $OH(A^2\Sigma^+)$ by N_2. The experiments can be grouped into six main categories: (I) experiments 1–10 were carried out under 'normal' conditions; (II) in experiments 11–13, the incident 248 nm laser power was varied; (III) in experiments 14 and 15, a known amount of N_2O was added to the photolysis mixture; (IV) in experiments 16–18, higher rotational states were excited (compared to the 'normal' experiments); (V) experiments 19 and 20 were 'blank' experiments designed to test the level of N_2O produced with both lasers turned off; (VI) experiments 21 and 22 were also 'blank experiments' in which Ar was employed instead of N_2 as the buffer gas. For each experiment a raw yield was computed as the number of N_2O molecules detected divided by the number of $OH(A^2\Sigma^+)$ molecules generated. Photolytically generated N_2O was taken to be the difference between the number of N_2O molecules detected in a given experiment and the number of N_2O molecules detected in a similar experiment where the dye laser was tuned off the OH absorption feature; for each set of operating conditions, at least one such 'off-line' experiment was carried out. The net N_2O yield is taken to be the number of photolytically generated N_2O molecules generated divided by the number of $OH(A^2\Sigma^+)$ molecules produced in the same experiment. Both the reported raw and net yields were corrected by multiplying them by 1.5. This correction accounts for the fact that a fraction of the $OH(A^2\Sigma^+)$ was quenched by H_2O. The mole fraction of H_2O in the photolysis mixtures was approximately 0.02; this mole fraction was deduced by pumping the $H_2O_2/H_2O/N_2$ gas mixture out of the photolysis cell through a liquid nitrogen trap, then expanding the condensible material back into the cell where its pressure could be measured. Based on literature values for the rate coefficients for quenching of $OH(A^2\Sigma^+)$ by N_2 [30,31] and H_2O [32,33], which are known quite accurately, we estimate that $65 \pm 10\%$ of the $OH(A^2\Sigma^+)$ was quenched by N_2 in a typical experiment.

As mentioned above, experiments 1–10 (Table 1) were carried out under 'normal' experimental conditions which were selected to optimize the chances of observing a very small photochemical yield of N_2O. In seven of these ten experiments the dye laser was tuned to the strong $Q_1(2)$ OH absorption line, while in the other three experiments it was tuned slightly off this line. In the seven experiments where $OH(A^2\Sigma^+)$ was excited, the observed net yields of N_2O ranged from $+2.9 \times 10^{-5}$ to -1.1×10^{-5}; the average net yield was $+0.6 \times 10^{-5}$. No significant dependence of the measured yield on dye laser power was observed.

Category II experiments showed that the number of N_2O molecules generated is independent of the excimer laser power. The rather large net yield obtained in experiment 12 results from the fact that relatively few $OH(A^2\Sigma^+)$ molecules were generated in that experiment.

The category III experiments verify that the photolysis, excitation, transfer, and detection processes could be carried out without *destroying* any photochemically generated N_2O. In both category III experiments, the amount of N_2O detected at the end of the experiment was (within the precision of the measurement) equal to the amount of N_2O added to the initial photolysis mixture. Category IV experiments were designed to investigate the effect of rotational excitation of $OH(A^2\Sigma^+)$ on the observed N_2O yield. The net N_2O detected from this set of experiments was found to be similar in magnitude to previous experiments carried out using the less rotationally excited $Q_1(2)$ line. Once again, however, both the raw and net N_2O yields were found to be somewhat larger than in most other experiments because relatively few $OH(A^2\Sigma^+)$ molecules were generated (because the $OH(X^2\Pi)$ rotational states being pumped had relatively small populations). Category V experiments examined the effect of turning both lasers off

on the number of N_2O molecules detected. The number of N_2O molecules observed in these experiments *is not statistically different from the* N_2O *levels observed in the other experiments*. The last set of experiments (category VI) used Ar instead of N_2 as the buffer gas. The net yield value of 2.1×10^{-5} is not significantly different from the yields obtained in the experiments with N_2 bath gas. Since in the presence of Ar it is not possible to form N_2O by reactions (2a) and (2b), it must be concluded that no statistically significant photochemical production of N_2O is observed in these experiments. Fig. 4 shows that there is no obvious correlation between the net N_2O detected and the amount of $OH(A^2\Sigma^+)$ generated in the N_2 buffer gas experiments, further strengthening the observation that very little, if any, of the N_2O detected was generated photochemically from reactions (2a) and (2b).

Based on our experimental results, the upper limit quantum yield for production of N_2O from the reactive quenching of $OH(A^2\Sigma^+)$ by N_2 is conservatively estimated to be 1×10^{-4}. This is the first time that a definitive upper limit yield has been placed on this reaction since the previous attempts were hampered by experimental difficulties. As discussed by Walkauskas et al. [27], experiments by Zipf [26] suggested that N_2O was formed by reactions (2a) and (2b) with a quantum yield of about 2%. H_2O/N_2 mixtures were photolyzed with vacuum-UV radiation from krypton and xenon resonance lamps for periods of 10 to 200 min. The products were then analyzed by gas chromatography to detect N_2O. This method of analysis could have led to artifact production of N_2O on various surfaces. Furthermore, due to the presence of high-energy radiation, not only could many reactive species have been formed, but photolysis of N_2O was also possible. Zipf attempted to deal with these complications by using a complex kinetic analysis, but the uncertainties associated with this method do not allow for a definitive determination of the N_2O quantum yield. In the second study of N_2O production via reaction (2b), Walkauskas et al. [27] generated OH radicals in a fast flow reactor by reacting hydrogen atoms with nitrogen dioxide, and excited OH to the $A^2\Sigma^+$ state using a powerful Xe/Hg arc lamp. The products generated in the flow reactor were trapped at a temperature of 77 K and transferred to a gas chromatograph-mass spectrometer for detection. Unfortunately, the background level of N_2O, i.e., the amount of N_2O that was detected in experiments with the Xe/Hg lamp off, was found to be in large excess over any N_2O generated photochemically. As a result, a meaningful N_2O yield from reactions (2a) and (2b) could not be determined.

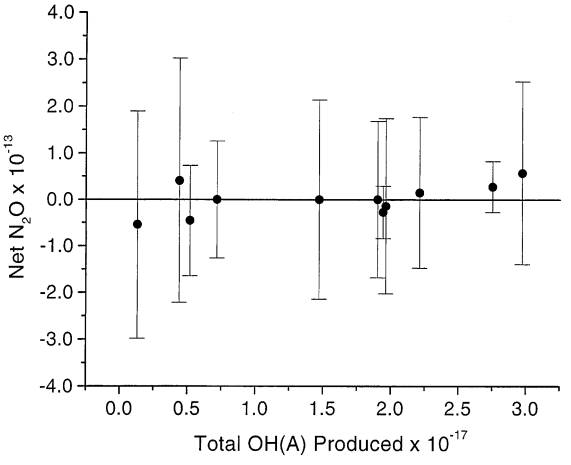

Fig. 4. Plot of net N_2O detected versus the total number of $OH(A^2\Sigma^+)$ generated in the N_2 buffer gas experiments. Error bars are 2σ and represent precision only.

As mentioned in Section 1, the reverse reaction of translationally hot H atoms with N_2O has been observed to yield OH $A^2\Sigma \rightarrow X^2\Pi$ chemiluminescence in three published studies [23–25]. These studies provided important motivation for this work in general, and for the experiments where $OH(A^2\Sigma^+)$ was rotationally excited in particular, since the $OH(A^2\Sigma^+)$ product of the reaction of translationally hot H atoms with N_2O is somewhat rotationally hot when the reaction is run under bulk conditions (all collision geometries possible) [23], and very rotationally hot when the reaction is initiated by photodissociation of a HBr–N_2O Van der Waals complex (precursor geometry limited conditions) [25]. In our experiments we did not attempt to excite $OH(A^2\Sigma^+)N'' > 7$, because the populations in the rotational states of $OH(X^2\Pi)$ from which absorption would have to occur in

order to access these states optically were too small. Of course, high rotational states of $OH(A^2\Sigma^+)$ are not produced by optical excitation of $OH(X^2\Pi)$ in the atmosphere. As discussed by Hoffmann et al. [23], reaction of $H(^2S)$ with $N_2O(X^1\Sigma^+)$ to produce $OH(A^2\Sigma^+) + N_2(X^1\Sigma_g^+)$ is nonadiabatic, i.e., both the forward and reverse reactions proceed via a surface-hopping mechanism. One plausible explanation why we obtain a negative result in spite of the fact that $OH(A^2\Sigma^+)$ chemiluminescence is readily observable from the reverse reaction is that the probability of a surface-hopping transition is optimized when $OH(A^2\Sigma^+)$ is vibrationally and/or rotationally excited. Another possibility, of course, is that even though $OH(A^2\Sigma^+)$ emission is readily observable in the translationally hot $H + N_2O$ studies, the yield of $OH(A^2\Sigma^+)$ is very small.

The most recent analysis of the atmospheric N_2O budget suggests that the input flux of N_2O into the atmosphere is approximately 4×10^{35} molecules per year [6]. To assess the potential importance of reaction (2b) as an atmospheric source of N_2O, an upper limit production rate via this reaction has been calculated. Using the best available OH absorption cross-sections [34] and solar intensities in the 300–320 nm wavelength region [35], the rate of excitation of $OH(A^2\Sigma^+)$ is calculated to be $\sim 4 \times 10^{34}$ per year in the troposphere (0–12 km) and $\sim 4 \times 10^{35}$ per year in the stratosphere (12–50 km). Allowing for the fact that about 40% of the $OH(A^2\Sigma^+)$ that is formed in the atmosphere is lost via quenching by N_2 [30–33], we conclude that $\sim 2 \times 10^{35} N_2O$ per year would be produced from $OH(A^2\Sigma^+) + N_2$ *if* the N_2O yield from this reaction was unity. Since we have demonstrated that the N_2O yield is less than 1×10^{-4}, the total atmospheric N_2O production rate via reactions (2a) and (2b) is less than 2×10^{31} molecules per year, i.e., less than 0.005% of the total atmospheric source strength.

Acknowledgements

This research was supported by the National Science Foundation (grant ATM-95-26510) and by the National Aeronautics and Space Administration (grant NAG5-8931). The authors thank S.S. Prasad for a number of helpful discussions and also thank H. Yu and S.C. Liu for calculating the atmospheric OH photoexcitation rate.

References

[1] R.E. Dickinson, R.J. Cicerone, Nature 319 (1986) 109.
[2] R.R. Garcia, S. Solomon, J. Geophys. Res. 99 (1994) 12937.
[3] World Meteorological Organization (WMO), Scientific Assessment of Ozone Depletion: 1998, Report No. 44, Global Ozone Research and Monitoring Project, Geneva, Switzerland, 1999.
[4] M.A. Khalil, R.A. Rasmussen, J. Geophys. Res. 97 (1992) 14651.
[5] A.F. Bouwman, K.W. Van der Hoek, J.G.J. Olivier, J. Geophys. Res. 100 (1995) 2785.
[6] C. Kroeze, A. Mosier, L. Bouwman, Global Biogeochem. Cycles 13 (1999) 1.
[7] Intergovernmental Panel on Climate Change (IPCC), Climate Change: Radiative Forcing of Climate Change and Evaluation of the IPCC IS92 Emission Scenarios, Cambridge University Press, Cambridge, UK, 1995.
[8] S.S. Prasad, J. Geophys. Res. 99 (1994) 5285.
[9] R.F. Delmdahl, K.-H. Gericke, Chem. Phys. Lett. 281 (1997) 407.
[10] E.C. Zipf, S.S. Prasad, Geophys. Res. Lett. 25 (1998) 4333.
[11] K.-R. Kim, H. Craig, Science 262 (1993) 1855.
[12] S.S. Cliff, M.J. Thiemens, Science 278 (1997) 1774.
[13] T. Rahn, M. Wahlen, Science 278 (1997) 1776.
[14] T. Rahn, H. Zhang, H. Wahlen, G.A. Blake, Geophys. Res. Lett. 25 (1998) 4489.
[15] S.S. Cliff, C.A.M. Brenninkmeijer, M.H. Thiemens, J. Geophys. Res. 104 (1999) 16171.
[16] D.W.T. Griffith, G.C. Toon, B. Sen, J.-F. Blavier, R.A. Toth, Geophys. Res. Lett. 27 (2000) 2485.
[17] Y.L. Yung, C.E. Miller, Science 278 (1997) 1778.
[18] C.E. Miller, Y.L. Yung, Chemosphere: Global Change Sci. 2 (2000) 255.
[19] T. Rockmann, C.A.M. Brenninkmeijer, M. Wollenhaupt, J.N. Crowley, P.J. Crutzen, Geophys. Res. Lett. 27 (2000) 1399.
[20] H. Zhang, P.O. Wennberg, V.H. Wu, G.A. Blake, Geophys. Res. Lett. 27 (2000) 2481.
[21] F. Turatti, D.W.T. Griffith, S.R. Wilson, T. Rahn, H. Zhang, G.A. Blake, Geophys. Res. Lett. 27 (2000) 2489.
[22] D. Krankowsky, P. Lammerzahl, K. Mauersberger, Geophys. Res. Lett. 27 (2000) 2593 (and references therein).
[23] G. Hoffmann, D. Oh, H. Iams, C. Wittig, Chem. Phys. Lett. 155 (1989) 356.
[24] E. Bohmer, S.K. Shin, Y. Chen, C. Wittig, J. Chem. Phys. 97 (1992) 2536.
[25] H. Ohoyama, T. Sawai, S. Tsuboi, T. Kasai, J. Chem. Phys. 109 (1998) 4443.

[26] E.C. Zipf, unpublished results.
[27] L.P. Walkauskas, L.G. Piper, B.D. Green, Physical Sciences Inc., Report PSI-945/TR-561 (1986).
[28] G.H. Diecke, H.M. Crosswhite, J. Quantum Spectrosc. Radiat. Trans. 21 (1962) 97.
[29] E.G. Estupinan, R.E. Stickel, P.H. Wine, Chemosphere: Global Change Sci. 2 (2000) 247.
[30] M.I. Lester, R.A. Loomis, R.L. Schwarts, S.P. Walch, J. Phys. Chem. A 101 (1997) 9195 (and references therein).
[31] A.E. Bailey, D.E. Heard, P.H. Paul, M.J. Pilling, J. Chem. Soc. Faraday Trans. 93 (1997) 2915.
[32] I.J. Wysong, J.B. Jeffries, D.R. Crosley, J. Chem. Phys. 92 (1990) 5218.
[33] A.E. Bailey, D.E. Heard, D.A. Henderson, P.H. Paul, Chem. Phys. Lett. 302 (1999) 132.
[34] R.P. Cageao, Y.L. Ha, Y. Jiang, M.F. Morgan, Y.L. Yung, S.P. Sander, J. Quantum Spectrosc. Radiat. Trans. 57 (1997) 703 (and references therein).
[35] H. Yu, S.C. Liu, personal communication.